Journal of Power Sources 187 (2009) 39–48

Contents lists available at ScienceDirect

Journal of Power Sources

journal homepage: www.elsevier.com/locate/jpowsour

Review of gas diffusion cathodes for alkaline fuel cells

F. Bidault[a], D.J.L. Brett[b], P.H. Middleton[c], N.P. Brandon[a,*]

[a] Department of Earth Science and Engineering, Imperial College London, UK
[b] The Centre for CO_2 Technology, University College London, UK
[c] Faculty of Engineering and Science, University of Agder, Grimstad, Norway

ARTICLE INFO

Article history:
Received 7 August 2008
Received in revised form
26 September 2008
Accepted 18 October 2008
Available online 5 November 2008

Keywords:
Alkaline fuel cell
Gas diffusion cathode
Electrode design

ABSTRACT

This paper gives a technical background to alkaline fuel cells (AFCs), introducing the advantages and drawbacks of the technology. AFCs offer the potential for low cost, mass producible fuel cells, without the dependency on platinum based catalysts and (currently) expensive membrane electrolytes. The AFC uses relatively low cost electrolytes based on aqueous bases such as potassium hydroxide. The inherent CO_2 sensitivity of the electrolyte can be addressed by filtering out the CO_2 from the air intake using a simple scrubber and periodically replacing the liquid electrolyte.

A review of the state-of-the-art in gas diffusion cathode development is given. The overall cell performance and stability is dominated by the behaviour of the cathode, leading to a focus of research effort on cathode development. The performance and durability of the gas diffusion electrode is very much dependent on the way in which the layer structures are fabricated from carbon and polytetrafluoroethylene (PTFE). The choice and treatment of the carbon support is of prime importance for the final catalytic activity. Noble metal and non-noble metal catalysts have been investigated and show good performance, however, more work is still needed on cathode durability to ensure the long term success of the alkaline fuel cell.

1. Introduction

Alkaline fuel cells (AFCs) were the first practical working fuel cell following the pioneering work of Bacon [1]. AFCs can realise a high overall electrical efficiency greater than most other fuel cell types [2]. Recently, a system consisted of a 6 kW stack connected to the grid showed an efficiency between 50 and 60% (LHV) [3]. The AFC was developed and studied extensively throughout the 1960s to the 1980s [4], prior to the emergence of the proton exchange membrane fuel cell (PEMFC), which has subsequently attracted most of the attention from developers. However, primarily because the predicted cost reduction in PEMFCs remains problematic, a resurgence of interest in AFCs has occurred in recent years [5–9]. The utilization of non-noble metal catalysts and liquid electrolyte makes the AFC a potentially low cost technology compared to PEMFCs, which employ platinum catalysts and specially engineered electrolyte materials. Cost analyses have shown that ambient air AFC systems, for mobile and low power applications, are less expensive than ambient air PEMFC systems, and that AFCs still have the potential of major improvements with modest investment [10,11].

Historically, four different types of AFC cells have been developed and a description of each has been given by Gulzow [10]. These can be summarised as follows: (i) cells with free liquid electrolyte, (ii) cells with liquid electrolyte in the pore-system, (iii) matrix cells where the electrolyte is fixed in the electrode matrix, and (iv) falling film cells. The one common aspect of these cells is that they all use porous electrode architectures which are similar to the electrode used in metal air batteries [12]. More recently, the alkaline anion-exchange membrane (AAEM) has attracted increasing attention [13–15]. The feasibility of an AAEM direct methanol fuel cell has been discussed, taking into account the thermodynamic disadvantage induced by the pH difference across the membrane, and kinetic advantages; it was concluded that the technology was worth further study [16]. The development of AAEM fuel cells have several important advantages over conventional AFCs: (i) since there is no mobile cation there is no precipitated carbonate, (ii) no electrolyte weeping, (iii) reduced methanol crossover, (iv) potentially simplified water management, due to the fact that the water is produced at the anode and consumed at the cathode, (v) a larger repertoire of effective catalyst materials, and (vi) potentially reduced corrosion [17]. However, while the AAEM fuel cell holds great promise, developments still need to be made to achieve suitably conducting and stable membranes.The anode electrode for AFCs has been less studied than the cathode, where catalyst containing platinum-group metals such as Pt/Pd has shown good performance and stability

* Corresponding author. Tel.: +44 20 7594 5704; fax: +44 20 7594 7444.
E-mail address: n.brandon@imperial.ac.uk (N.P. Brandon).

0378-7753/$ – see front matter © 2008 Elsevier B.V. All rights reserved.
doi:10.1016/j.jpowsour.2008.10.106

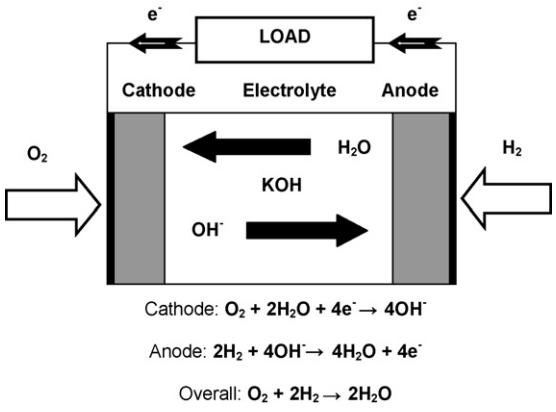

Fig. 1. Diagram showing the fundamentals of an alkaline fuel cell.

[18,19]. Nickel has also been studied as a potential low cost catalyst for AFCs anodes [20,21]. Raney nickel, which offers the advantage of high surface area, has been shown to be one of the most active catalysts for the hydrogen oxidation reaction in alkaline media, but has reported to suffer from deactivation [22–24] which could be improved by the addition of copper [25] or treatment with H_2O_2 [26].

The power output and lifetime of alkaline fuel cells are directly linked to the behaviour of the cathode, where most of the polarization losses occur, because the oxygen reduction reaction (ORR) is a slow reaction compared with hydrogen oxidation reaction at the anode. As a consequence, cathode development requires special attention to find the best catalyst and electrode structure to combine performance and stability. After a brief technology background, this review focuses on the state-of-the-art gas diffusion cathode materials and designs used with circulating electrolyte AFCs.

2. AFC technical review

In an alkaline fuel cell (Fig. 1), hydroxyl ions are produced at the cathode and migrate to the anode side where they react with hydrogen. Some of the water formed at the anode diffuses to the cathode and reacts with oxygen to form hydroxyl ions in a continuous process. The overall reaction produces water and heat as by-products and generates four electrons per mole of oxygen, which travel via an external circuit producing the electrical current.

The use of a non-noble metal catalyst is possible because the oxygen reduction reaction in alkaline media is more facile than in acid media. As a consequence, higher voltages at a given current density can be obtained, leading to a higher electrical efficiency [4].

The main disadvantage of AFCs is that carbon dioxide can react with the electrolyte to form carbonate Eq. (1), decreasing the electrolyte conductivity, oxygen solubility and electrode activity. The formation of precipitated carbonate Eq. (2) can also lead to the blockage of the electrolyte pathways and electrode pores.

$$CO_2 + 2OH^- \rightarrow {CO_3}^{2-} + H_2O \quad (1)$$

$${CO_3}^{2-} + 2K^+ \rightarrow K_2CO_3 \quad (2)$$

Potassium hydroxide solution (KOH) is almost exclusively used as the electrolyte because it has a higher ionic conductivity than sodium hydroxide solution, and potassium carbonate has a higher solubility product that sodium hydroxide, which renders the former less likely to precipitate [27].

In most terrestrial applications, the KOH electrolyte is circulated through the stack, which has some advantages over the alternative immobilized systems which have been favoured in space applications such as Apollo and the Space shuttle. The use of a circulating electrolyte allows thermal and water management to be easily controlled. Moreover, impurities (e.g. carbon from electrodes or carbonates) can be easily removed, making the circulating electrolyte systems less sensitive to CO_2 poisoning than the immobilized electrolyte systems. The OH^- concentration gradient is also greatly decreased and the build up of gas bubbles in the gap between the electrodes minimized [28]. However, electrolyte leakage and parasitic losses are challenging problems and need to be carefully considered by developers. The main advantage of the immobilized systems is the simplicity of construction and the ready removal of product water from the hydrogen side of the system. However, such systems are very prone to degradation of the electrolyte due to impurities, and require very pure hydrogen and oxygen to function reliably. Because of this, they are ideally suited for space applications where tanked hydrogen and oxygen are used for propulsion.

As a consequence of the CO_2 sensitivity, AFCs have tended to be demonstrated in special applications where pure hydrogen and pure oxygen are provided, such as space. In such systems the KOH electrolyte has been immobilized in a matrix constructed from thin asbestos sheets. Asbestos is the preferred material in this application due to its exceptional stability and absorption properties. The use of a porous matrix, soaked with KOH, which allows the elimination of moving parts, was developed by NASA. Bacon's invention of the double-layer sintered electrode made from nickel powder was the starting point of this technology, which led to its use as the electrical power source in the Apollo missions to the moon and later in the shuttle Orbiter. The Orbiter fuel cell system, which operated at 4 atmospheres and 95 °C, was manufactured by United Technologies Corp, (UTC) Fuel Cells. The system has given impressive performance up to 470 mA cm^{-2} at 0.88 V. However, in order to achieve this performance, the electrodes required a high noble metal loading of 10 mg cm^{-2} at the anode (80% Pt–20% Pd), and 20 mg cm^{-2} at the cathode (90% Au–10% Pt) [29].

Alkaline fuel cells were the first fuel cell technology to be put into mobile applications through its demonstration as the power source for a farm tractor in the late 1950s by Allis Chalmers. Union Carbide Corp. (UCC) developed circulating electrolyte systems leading to the demonstration of Kordesch's Austin A 40 fuel cell car for several years on public roads in the early 1970s [4,30].

In more recent years, AFC companies such as Zetek [31,32] focused on the design of circulating electrolyte low temperature unpressurised systems for backup power, stationary and mobile applications. The aim was to achieve a low cost mass production fuel cell. Injection-moulded plastic frames (usually polypropylene), which house the electrodes, were used to build the stack. Each frame was friction welded to the next to ensure that the stack was leak-free. Low cost electrode production was ensured by the use of standard industrial processes such as rolling (calendaring) and pressing.

The electrolyte of choice for terrestrial applications running on air and industrial grade hydrogen is 30–40% KOH, circulated though the stack with a pump. This has the advantage of allowing easy replacement when CO_2 absorption has reached an unacceptably high level. Moreover, circulating electrolytes provides a very effective way of cooling the stack and heat recovery via a heat exchanger. The system is designed to be as simple as possible as outlined in (Fig. 2).

The electrolyte circulation loop consists of a KOH tank, a KOH pump and a heat exchanger. During start up the KOH is heated to the desired operating temperature, typically 70 °C. During operation the heat exchanger is used to remove excess heat. This can be recov-

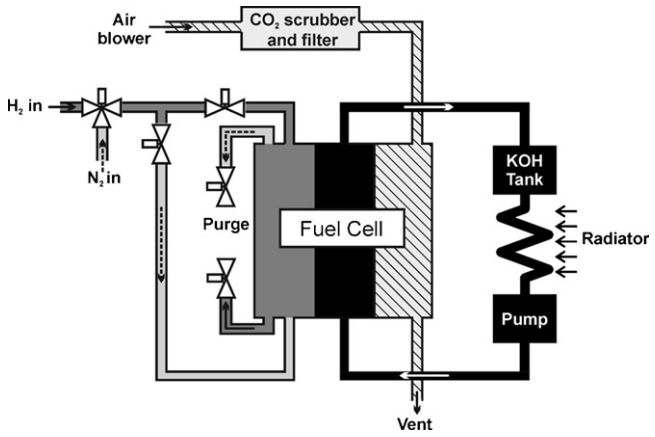

Fig. 2. Schematic of a circulating electrolyte alkaline system.

ered for space heating applications. An air blower forces air into a CO_2 scrubber (usually containing soda lime), from where the air is directed to the air-intake. McLean estimates the cost of the scrubbing using soda lime between 0.2 and 2.6 Dollar cents/kWh [10]. The outlet air is directly exhausted to the atmosphere whereas the hydrogen is re-circulated or dead ended for maximum efficiency. The hydrogen circulation is achieved by means of a jet pump which facilitates the evacuation of the excess water that is collected in a water trap. The start-up/shut-down procedure is quick and easily performed by means of a nitrogen purge [32–34].

Both monopolar [31,32] and bipolar stack designs [6,34] have been demonstrated. The monopolar stack design (Fig. 3) presents several advantages: (i) low cost due to the avoidance of expensive bipolar plates, (ii) stack thickness decreases as there is only one gas chamber between two electrode, (iii) no mechanical pressure is required because cells are usually glued or welded, (iv) modularity of the power delivered by changing the external current connectors and (v) the disconnection of a bad cell facilitates maintenance of the stack [28]. However, the monopolar design is limited to a current density of up to 100 mA cm^{-2} due to the losses associated with current collection on the side of each electrode. By contrast, the bipolar design demonstrates a uniform current density over all of the electrode surface and higher terminal voltage with less power limitation, and is therefore the preferred geometry for high power applications [34].

Typical AFC performance obtained at different temperature and pressure are given in Fig. 4.

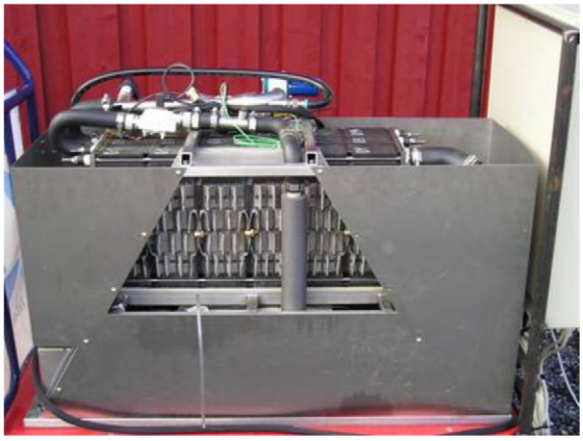

Fig. 3. Picture of a monopolar Zetek stack (University of Agder).

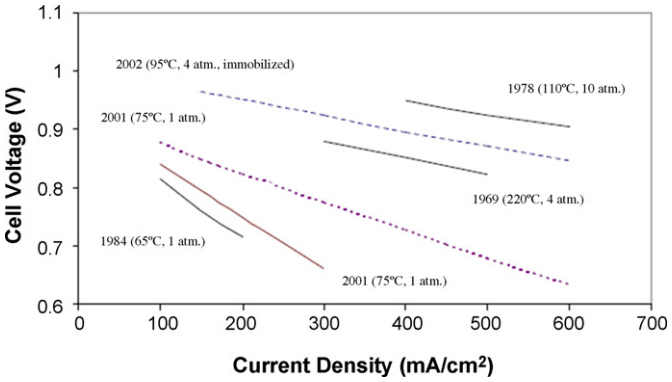

Fig. 4. Evolution in AFC system performance: H_2/air performance is shown as solid lines and H_2/O_2 performance is shown as dashed lines [29].

A 20,000 h life time of accumulated module operation has been achieved by Siemens using a Ni-anode and Ag-cathode [33] and 15,000 h with a shorter stack than usually used in the space-shuttle by UTC [2]; however, this performance data was obtained with pure oxygen and hydrogen. When air is supplied to the system, even with scrubbing a large part of the CO_2, lifetime is much less. A stack made by Zevco has been reported to have delivered power for 5000 h using low platinum loading and a circulating electrolyte system [32]. Insufficient studies have been done to date and the durability of AFC systems remains a key issue, especially when using non-noble metal catalysts and air.

3. AFC gas diffusion cathode

3.1. Electrode design

In general, AFC electrodes consist of several PTFE-bonded carbon-black layers, which fulfil different functions. The three-layer electrode structure shown schematically in Fig. 5, consists of a backing material (BM), a gas diffusion layer (GDL) and an active layer (AL). This design is preferentially used over single layer electrodes [35]. More complex electrode designs with more than three layers have been reported, for example, two different GDLs on top of each other and an AL, however such geometries are rare [28].

The BM should have a high permeability to gases, high structural strength, good corrosion resistance and high electronic conductivity. In a monopolar design, the BM serves as the current collector, so metal screens, meshes or foams, usually made of nickel, are generally used. In bipolar designs, the BM is in direct contact with the bipolar plate. This means the BM can also be made of carbon cloth or porous carbon paper in a similar way to the design of PEM fuel cells [34].

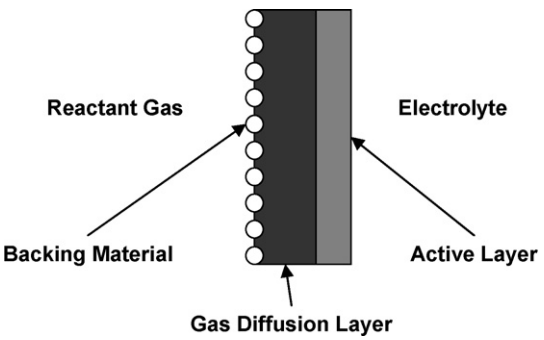

Fig. 5. Design of a double layer electrode for a bipolar stack design.

The GDL supplies the reactant gas to the AL and prevents the liquid electrolyte from passing through the electrode. This effect is often termed 'weeping'.

Monopolar designs almost exclusively use a GDL made from porous PTFE. The porosity is achieved by mixing the PTFE suspension with sugar or ammonium carbonate. When sintered at elevated temperature, the ammonium carbonate filler decomposes, producing gas bubbles which create porosity in the PTFE film [36]. Bipolar designs require a GDL that is electronically conducting. This precludes using pure PTFE and instead favours mixtures of PTFE with conducting carbon support [37]. The ratio of carbon/PTFE (25–60% PTFE) is a trade-off between the level of hydrophobic behaviour of the PTFE and the conductivity of the carbon support. Ideally the GDL should be completely water repellent and of metallic conductivity.

The active layer (AL) contains the catalyst which is usually supported on carbon black and bonded together with PTFE. The carbon black is chosen to have a high surface area to maximise the power density. The level of PTFE in the AL is less than in the GDL, typically the AL will contain between 2 and 25% PTFE, depending on the level of hydrophobicity required. The basic function of the PTFE in the active layer is to bind the carbon black together, but still provide multiple three-phase contact points where gas, electrolyte and carbon supported catalyst meet [38]. Different structures depending on the nature of the carbon support, carbon/PTFE ratio and electrode fabrication process can be obtained where electronic conductivity, ionic transport and gas transport have to be provided [39].

3.2. Materials used in electrode fabrication

AFC electrodes can be made of different materials with different structures, but modern electrodes tend to use high surface area carbon supported catalysts and PTFE to obtain the necessary three phases boundary (TPB). Electrode performance in AFCs depends on catalyst surface area rather than catalyst weight. As with all other fuel cells, the catalyst loading is a critical parameter in determining performance. The nature of the catalyst support is also of prime importance to achieve high catalytic activity.

PTFE is a hydrophobic polymer material which has become the binding agent of choice since its commercial introduction in the 1950s by Dupont; although other materials are sometimes used (paraffin, polyethylene, polypropylene, wax etc.). It is available either as dry powder additives, or as a ready made aqueous suspension (containing proprietary dispersants). Both of these forms have been used to make electrodes [39]. PTFE can be present in the form of spherical particles, fibrils or thin films on porous substrates [40]. The PTFE penetrates deep into the sub-surface of the carbon when the dispersion is mixed with the carbon black powder. However, generally it is necessary to melt the PTFE in order to provide a thin film over the entire surface of the carbon black. This process is usually called sintering and takes place at temperatures around 320 °C [41,42].

The electrical, chemical and structural properties of carbon make it an ideal material for use in AFC electrodes [43]. Carbon blacks, which are the most commonly used carbon support in AFC electrode fabrication, consist of carbon in the form of near spherical particles obtained by the thermal decomposition of hydrocarbons. High surface area is achieved in a separate step, by treatment with steam at a temperature in the range of 800–1000 °C. The inner core of the carbon particle is less ordered than the outside, and as a consequence the action of the steam causes large numbers of pores to form which interconnect to create the characteristic high surface area. The particle, however, does not completely disintegrate, but remains agglomerated to its neighbours. Specific surface areas of over 1000 $m^2 g^{-1}$ can be obtained [44]. Porosity and surface area are the main characteristics of the carbon black structure. Studies have been carried out in order to gain better control of the carbon structure during the fabrication process [45]. Oxygen and hydrogen groups are introduced onto the carbon surface during the manufacturing process. The carbon-oxygen group is by far the most important and influences the physico-chemical properties of carbon blacks. Chemisorption of oxygen, and a build-up of carbon-oxygen surface compounds, occurs at temperatures below 400 °C, whereas decomposition of these compounds occurs above 400 °C. Formation of these groups by oxidative treatment in gaseous and liquid phases has been comprehensively studied [44,46].

Despite the preference to use carbon black in gas diffusion electrode (GDE) fabrication, alternative catalyst supports have been tried. Hacker reported similar performance between silver and platinum catalysts supported on carbon nanofibres showing the capability of the fibres to provide the required porosity and pore structure to obtain good performance [47]. Huang showed higher performance using a binary catalyst support composed of carbon nanotubes (CNT) and active carbon black compared with a single-support catalyst. The best performance was obtained when the mass ratio was 50:50 [48]. Yang also showed good electrochemical performance with the same kind of binary support using MnO_2 as catalyst. A higher accessible surface area, an improved conductivity, and faster ORR kinetics explain the improvement [49]. Carbon nanotube/perovskite composite materials have also been tested by Weidenkaff with promising results [50].

3.3. Operational mechanism

The electrochemical behaviour of the GDE can be controlled by varying the structure of its component layers and in particular by varying the ratio of hydrophobic and hydrophilic pores within the carbon support. Two structures have been developed, each playing a different role within the electrode. The primary 'macro' structure is formed at distances greater than 1 μm, and is created by the partial enclosure of the carbon particles by the PTFE. It forms the skeleton structure which ensures electronic conductivity throughout the electrode and also provides mechanical support. Different macrostructures can be obtained by varying the carbon particle size and shape, the carbon/PTFE ratio, and the electrode fabrication process. The secondary 'micro' structure, created by the pore system inside of the carbon particles, depends on the surface area and pore structure of the carbon used. This structure is directly linked to the carbon manufacturing and activation process which greatly influences the micro-porosity of the carbon particles [39]. Indeed, the carbon particles have been shown to consist of macropores which are hydrophobic, and micropores (<0.01 μm) which are hydrophilic. The hydrophilic and hydrophobic property of the carbon depends on the nature of the surface groups which can be selected by various thermal and chemical treatments. The hydrophobic macropores have been shown to play an essential role in gas mass-transport by acting as gas supplying channels. The ORR mechanism occurs in the hydrophilic micropores which are filled with electrolyte and on the boundary of micro and macropores [51,52].

The TPB is formed in the outer regions of the carbon particle shell where it is covered by a film of liquid electrolyte at the interface between the carbon micro and macro structures. The carbon particles arrangement is described as a 'tight bed of packed spheres' where the large vacancies between the particles are filled with electrolyte ensuring the ionic transport and where the carbon pore system and hydrophobic channels created by the PTFE ensure the gas transport as shown in Fig. 6 [39].

The thicknesses of the different layers have to be controlled to optimise electrode performance. The GDL thickness has to be as

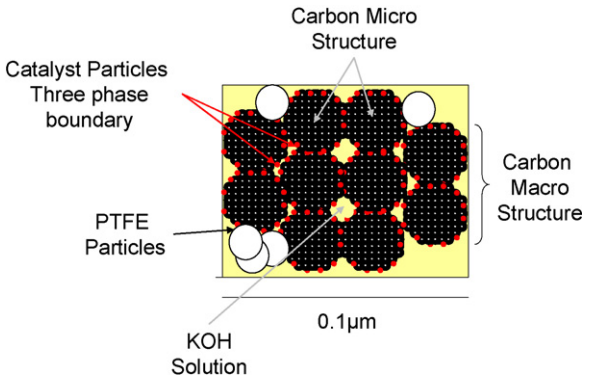

Fig. 6. Schematic illustration of the carbon macro and micro structure within the active layer.

thin as possible to maximise oxygen accessibility, while the AL has to be optimized to maximise the reaction area constituted by the TPB. Kiros obtained maximum limiting current densities with two different catalysts, the AL thickness lying between 0.5 and 0.6 mm [53].

3.4. Electrode modelling

Many publications have discussed the behaviour of porous electrodes in alkaline fuel cells. Whereas some authors have focused on specific issues such as current distribution [54], or the degree of catalyst utilization [55,56], the majority have tried to understand the overall mechanism of operation in the GDE related to the structure; considering factors such as gas diffusion and electrolyte penetration. Several models have been used such as the simple pore model [57], the thin film model [58] or the dual scale of porosity model [59]. In the former, a range of porosities is considered, where macropores are gas filled and micropores are electrolyte filled [60,61]. Giner [62] listed the limitations of this 'flooded porous electrode' model introducing the concept of 'flooded agglomerates'. The operational mechanism of this structure, shown in Fig. 7, consists of catalyst particles which form porous agglomerates 'flooded' with electrolyte under working condition. The agglomerates are kept together by the PTFE which creates hydrophobic gas channels. Reactant gases diffuse through the channels and dissolve in the electrolyte contained in agglomerates to react on available catalyst sites. It has been reported elsewhere that the concept of 'flooded agglomerates' gives a satisfactory explanation for the behaviour of PTFE-bonded gas diffusion electrodes, and is in good accordance with experimental findings [40,63–65].

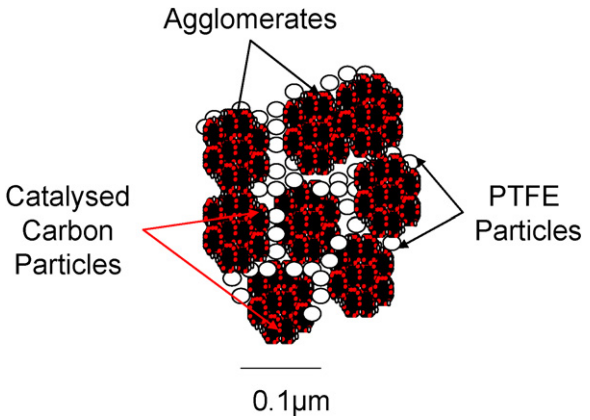

Fig. 7. Schematic illustration of the 'flooded agglomerate' model.

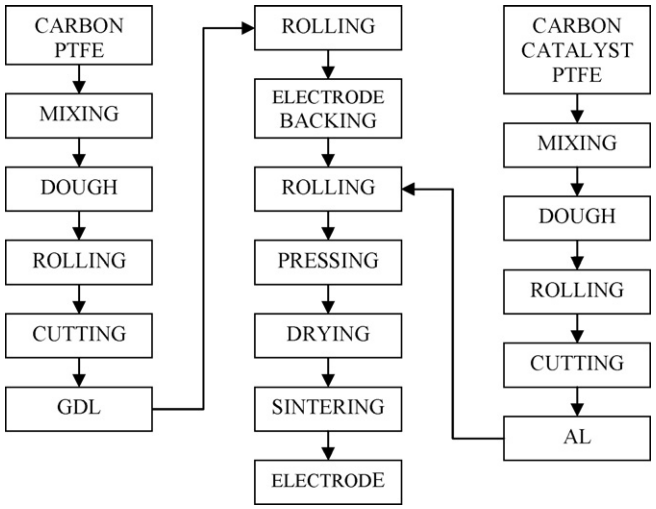

Fig. 8. Electrode fabrication: the rolling method.

Further single cell (anode/electrolyte/cathode) models have shown that cathode reaction kinetics are particularly important in determining the overall cell performance, predicting that the diffusion of dissolved oxygen contributes most to the polarization losses at low potentials (high current region), while the electronic resistance contributes most at high cell potentials (low current region). As a consequence, cell performance can be increased by means of improved cathode fabrication methods, in which both gas-liquid and liquid-solid interfacial surface areas are increased and the diffusion path of dissolved oxygen to catalytic sites is reduced [30,56,66–68].

3.5. Electrode fabrication

Since different electrode structures lead to different cathode performance, the electrode fabrication requires special attention where the gas permeability of the GDL and the wettability of the AL are the two main performance-limiting factors [69]. Structural parameters of the different layers can to be optimized by varying the carbon support used, the carbon/PTFE ratio and the fabrication conditions to obtain the best cathode performance [12,39,70–72]. The electrochemical performance of the electrodes is also controlled by the initial porous structure and chemical surface properties of the active carbon, which in turn depend on the process fabrication route. An activation step appears to improve the electrochemical activity and stability of the carbon black by means of thermal, physical and chemical treatments [73,74]. Increased surface area, formation of a defined inter-pore structure and an increased surface activity by the formation of catalytically active groups on the surface occurs during such treatment. The activity of carbon black is proportional to its surface area, the higher the better [75]. High temperature treatment leads to a higher surface area and as a consequence to a higher electrochemical activity. Carbon pre-treatment needs to be specific to the type of carbon black. For example, the surface area has been found to increase significantly for Vulcan XC-72 in the presence of CO_2, whereas a N_2 atmosphere is required for Ketjenblack when heat-treated at 900 °C [76].

Pressing, rolling, screen-printing and spraying methods are used in the production of AFC electrodes [72,77]. The rolling method is the most commonly applied. The process shown in Fig. 8 is generic and variations include addition of filler materials such as sugar or ammonium bicarbonate, along with various washing or drying steps. If PTFE powder is used and ground with the carbon, the method is referred to as the 'dry-method'. If PTFE suspension

and water are mixed with the carbon black it is referred to as the 'wet-method' [71].

The method of mixing the carbon black with the PTFE will have a direct effect on the electrode activity and stability. Musilova showed that using an aqueous PTFE deposition process onto the carbon surface leads to a hydrophobic blend. However, if ethanol is used instead, the electrode is more hydrophilic [78]. Motoo and Watanabe showed that very fine networks of gas channels are needed in the AL to obtain high performance. Since diffusion of dissolved reactant gas is a limiting factor for high current generation, good dispersion of the carbon and PTFE particles is required to increase the number of gas dissolving sites and reduce the diffusion path length of dissolved gas to the catalyst sites, resulting in a performance increase. To achieve this, new techniques of fabrication have been applied involving, for example, colloid mill and ultrasonic agitation [79–81].

3.6. The oxygen reduction reaction (ORR) in alkaline media

Optimizing the cathode performance is essential because it governs the overall performance of the fuel cell. According to Bockris at high current density, 80% of the polarization may be due to the oxygen reduction [2]. The ORR is a complex process involving four coupled proton and electron transfer steps. Several of the elementary steps involve reaction intermediates leading to a wide choice of reaction pathways. The exact sequence of the reactions is still not known, and identification of all reaction steps and intermediates, and their kinetic parameters is required, which is clearly challenging. Appleby has reviewed and discussed the issues relating to the ORR in acid and alkaline solution [82]. In acid electrolyte, the ORR reaction is electrocatalytic, as pH values become alkaline, redox processes involving superoxide and peroxide ions start to play a role and dominate in strongly alkali media. The reaction in alkaline electrolytes may stop with the formation of the relatively stable HO_2^- solvated ion, which is easily disproportionated or oxidized to dioxygen. Although there is no consensus on the exact reaction sequence, two overall pathways take place in alkaline media [83]:

(i) Direct 4-electron pathway

$$O_2 + 2H_2O + 4e^- \rightarrow 4OH^- \quad (3)$$

Peroxide pathway or '2 + 2-electron' pathway:

$$O_2 + H_2O + 2e^- \rightarrow HO_2^- + OH^- \quad (4)$$

With

$$HO_2^- + H_2O + 2e^- \rightarrow 3OH^- \quad (5)$$

The peroxide produced may also undergo catalytic decomposition with the formation of dioxygen and OH^-, given by:

$$2HO_2^- \rightarrow 2OH^- + O_2 \quad (6)$$

The kinetics of the ORR reaction is more facile in alkaline medium than in some acid medium such as H_2SO_4 [84]. This is also illustrated by the comparison made by Blurton [85] for the operating potentials of a fuel cell running on H_2/O_2 at a controlled current density of 100 mA cm^{-2} at 70 °C with platinum electrodes. These workers reported a potential of 0.67 V for 13.9 M H_3PO_4 and a potential of 0.89 V for 6.9 M KOH versus a hydrogen reference electrode. The higher voltage (performance) of the alkaline system was explained by the preferred formation of peroxide species in the alkaline medium which desorbs more readily than in the acid counterpart.

Blizanac [86] used a thermodynamic analysis to explain the origin of the pH effect, showing that the overpotential required to facilitate the 4-electron transfer process at high pH is relatively small compare to the potential required at low pH in the case of Ag(111). At high pH, no specific chemical interaction between the catalyst and O_2 or O_2^- is required, whereas strong chemical interaction is necessary at low pH. Blizanac also explained how the low activity of catalysts in acid media is exacerbated by the presence of spectator species adsorbed onto the electrode surface, which act to physically block the active sites and also lower the adsorption energy for intermediates, so retarding the reaction rate.

3.7. Cathode catalyst materials

Due to the inherently faster kinetics for the ORR in alkaline media, a wide range of catalysts have been studied including noble metals, non-noble metals, perovskites, spinels, *etc.* However, it is important to appreciate that the carbon support plays a role in the kinetics as well as the catalyst supported on its surface, so that in evaluating the performance, it is necessary to assess the loading of the catalyst and the type of carbon used where its hydrophobic properties as well as its surface groupings greatly affect the final hydrophobic structure and the TPB length of the electrode. The performance of the catalyst/support system is considered since carbon participates in the reaction by a 2-electron process. The catalytic activity of the system is directly linked to the physical and chemical characteristics of the carbon support. The catalyst deposition method is critical since a high catalytic activity relies on a very fine and well dispersed catalyst particle. In the case of platinum, the particle size is generally in the nanometre range. The carbon impregnation of metal salt solution with further reduction of the metal is commonly used, and well known for it simplicity and ability to produce metal nanoparticles with nearly mono-dispersed size distribution and easy scale-up.

3.7.1. Noble metal catalyst

Platinum is the most commonly used and active catalyst for the electro-reduction of oxygen and all of the platinum-group metals reduce oxygen in alkaline media according to the direct 4-electron process [87–95]. At a very low Pt/C ratio, the overall number of electrons exchanged is approximately two due to the carbon contribution, but increases as the Pt/C ratio increases, reaching four electrons at 60% wt.Pt [96]. Pt-based alloys have been studied and generally exhibit higher activity [97] and stability [98] than Pt-alone. The enhanced electrocatalytic activity of Pt-alloy systems has been explained by a number of phenomena, including: (i) reduction in Pt–Pt bond distance, favouring the adsorption of oxygen; (ii) the electron density in the Pt 5d orbital and (iii) the presence of surface oxide layers [96,99–102]. Due to the high cost of Pt, techniques have been developed to reduce loading [56,96,102–104]. For example, monolayer deposition of Pt on non-noble metal nanoparticles showed improved catalytic properties with a very small amount of Pt [104,105]. The carbon impregnation with hexachloroplatinic acid solution ($H_2PtCl_6.6H_2O$) followed by metal reduction using heat treatment or wet chemical methods, have been widely used to produce a catalyst particle size lying between 12 and 34 nm [48,78,96,106,107]. A more complex colloidal precursor deposition technique showed a PtRu particle diameter close to 2 nm [108,109].

Silver has been studied as a potential replacement of Pt due to its high activity for the ORR and its lower cost. Silver in alkaline solutions is oxidized in two steps; first a layer of Ag_2O is formed which is partly oxidized in the second to AgO [110]. ORR occurs with the participation of 2 and 4-electron processes, depending on the surface state and in particular on its oxidation state and electrode potential [47,111–119]. The size of the Ag particles affects the different catalytic activity for these two processes. Four electrons are exchanged during ORR on nano-dispersed silver particles on

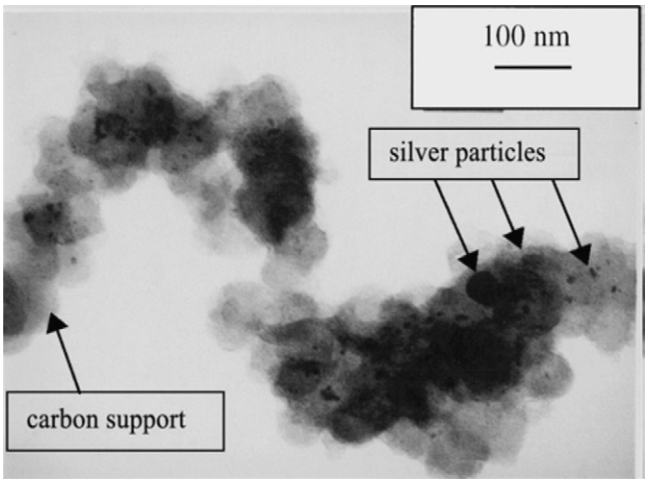

Fig. 9. TEM photograph for reduced carbon-supported silver nanoparticles [110].

carbon, with an optimum loading lying between 20 wt% [112] and 30 wt% [114]. The effect of electrolyte concentration is positive for silver catalyst but not for Pt catalyst, which is slightly hindered due to greater absorbed species coverage. Silver becomes competitive to Pt due to favoured kinetics in high concentration alkaline media [47,111], but shows a strong propensity to dissolution at open circuit voltages following Eq. (7) [28]:

$$4Ag + O_2 + H_2O \rightarrow 4Ag^+ + 4OH^- \quad (7)$$

At an overpotential of 100–300 mV, this dissolution was found not to be significant [114]. The impregnation of $AgNO_3$ is commonly used, associated with different techniques of Ag reduction [47,120]. Chatenet using impregnation of $AgNO_3$ and electrochemical reduction in sulphuric acid to obtain silver particle sizes in the range 5–10 nm (Fig. 9) [111].

3.7.2. Non-noble metal catalyst

Whereas carbon supports show poor electrochemical activity in acidic media [121], carbon blacks and graphite have been shown to catalyse the ORR in alkaline media with the formation of HO_2^- in a two electron process Eq. (2), where high surface area carbon blacks such as Vulcan XC-72R (25 nm, 250 $m^2\,g^{-1}$) showed an increased activity [74,75,121–123].

Recently, manganese oxides have attracted more attention as potential catalysts for both fuel cells [124,125] and metal-air batteries [126] because of their attractive cost and good catalytic activity toward O_2 reduction. The investigation of different manganese oxides dispersed on high surface area carbon black showed low activity for MnO/C and high activity for MnO_2/C and Mn_3O_4/C. The higher activity of MnO_2 was explained by the occurrence of a mediation process involving the reduction of Mn(IV) to Mn(III), followed by the electron transfer from Mn(III) to oxygen. The reaction was sensitive to the manganese oxide/carbon ratio in which, at lower ratios, the reaction proceeds by the 2-electron pathway, evolving to an indirect 4-electron pathway with disproportionation of HO_2^- into O_2 and OH^- at higher catalyst/carbon ratios [126–129]. The catalytic activity for the disproportionation reaction has led to a new approach of dual system catalysis in which one catalyst is used for the reduction of O_2 through the two-electron process producing HO_2^-, which is subsequently decomposed by MnO_2, leading to a four-electron process [130–132]. The MnO_2 catalytic activity was found to vary following its crystalline structure in the sequence: β-MnO_2 < λ-MnO_2 < γ-MnO_2 < α-MnO_2 ≈ δ-MnO_2, in which higher activity seems to go with higher discharge ability, proceeding through chemical oxidation of the surface Mn^{3+} ions generated by the discharge of MnO_2 rather than through a direct 2-electron reduction [133]. γ-MnOOH exhibits higher activity than γ-MnO_2; this has been explained by the fact that amorphous manganese oxide has more structural distortion and is more likely to have active sites compared to crystalline manganese oxides [126,134].

Pyrolysed macrocyles on carbon supports have been studied in alkaline media showing high activity towards the ORR. Cobalt phthalocyanine has been shown to reduce oxygen with similar kinetics to that of Pt [135]. Electrodes made of Cobalt/Iron tetraphenylporphyrin (CoTPP, FeTPP) demonstrated good performance, outperforming electrodes made of silver catalysts. Structural changes and increased surface area is required to enhance the catalytic activity, which is obtained by chemical and heat treatment of the carbon and the porphyrins [37,71,136]. This high catalytic activity was attributed to the combined effect of the macrocycle black and Co; however, poor stability has been shown where the loss of Co appeared to be important, leading to performance deterioration [137]. $CoCO_3$ + TetraMethoxyPhenylPorphyrin (TMPP) + carbon showed better performance than CoTMPP + carbon confirming the fact that the structure of the metal macrocycle is not responsible for catalytic activity, but its origin is due to the simultaneous presence of the metal precursor, active carbon and a source of nitrogen, supposed already to be part of the catalytic process [138,139].

Perovskite-type oxides, which have an ABO_3-type crystal structure, have shown a high cathode activity in alkaline media proceeding by a 2-electron pathway where HO_2^- is further reduced [140]. Good performance has been reported with different catalyst composition such as $La_{0.5}Sr_{0.5}CoO_3$, $La_{0.99}Sr_{0.01}NiO_3$ [141], $La_{1-x}A_xCoO_3$ (A = Ca, Sr) [142], $Ca_{0.9}La_{0.1}MnO_3$ [143] and $Pr_{0.6}Ca_{0.4}MnO_3$, $La_{0.6}Ca_{0.4}CoO_3$ [144]. The catalyst support choice seemed to be crucial to obtain stable performance. Graphite supports appeared less stable [145] than high surface area carbon black [140].

A spinel is a ternary oxide with an AB_2O_4 structure in which the choice of the B cation is critical since it plays an important part in the activity of the catalyst [146,147]. Studies of $MnCo_2O_4$ catalysts have mainly indicated an ORR mechanism that involves a 2-electron process with HO_2^- formation [148,149]. The catalytic activity depends greatly on the preparation route; the decomposition of Co and Mn nitrates and subsequent heat treatment is most commonly used [150–152].

3.8. Performance

A summary of the data in the literature describing cathode performance for different catalysts is given in Tables 1 and 2, which have been separated according to whether the measurements were made in oxygen or air. All the potentials are reported against an Hg/HgO reference electrode, the KOH concentration lying between 5 and 8 M. The electrolyte temperature varied between 25 and 70 °C and is reported for each instance.

3.9. Electrode durability

Several degradation rates have been reported; Tomantschger reported performance degradation under working conditions of 10–30 mV/1000 h over a period of 3500 h at 0.1 A cm^{-2} [141]. Gouerec showed a degradation rate of 5–10 mV/1000 h over a period of 2800 h at 0.1 A cm^{-2} [19]; Gulzow reported, over 3500 h at 0.15 A cm^{-2}, a degradation rate of 17 mV/1000 h with silver based electrodes [139]. Several causes or effects have been proposed to explain the degradation of AFC cathode performance with time; they are described in the following sections. The understanding of these effects and their studies is very important in the develop-

Table 1
Cathode performance using different catalysts with O_2.

Catalyst	KOH Temperature (°C)	KOH Concentration (M)	Potential vs. Hg/HgO (V)	Current Density (mA cm^{-2})	Source
Pt/Pd/C 4wt.%Pt/6wt.%Pd	25	6	−0.1	900	[153]
			−0.2	1600	
			−0.3	2100	
Ag/C 47 mg cm^{-2}	70	7	−0.1	250	[118]
			−0.2	540	
$La_{0.5}Sr_{0.5}CoO_3$/C 7%wt	25	6	−0.1	250	[141]
			−0.2	700	
			−0.3	1600	
CoTPP/C 1.76 mg cm^{-2}	40	5	−0.06	150	[37]
			−0.14	600	
			−0.18	950	
$La_{0.6}Ca_{0.4}CoO_3$/C 9–13 mg cm^{-2}	25	6	−0.1	150	[145]
			−0.2	500	
			−0.3	1000	

Table 2
Cathode performance using different catalysts with air.

Catalyst	KOH Temperature (°C)	KOH Concentration (M)	Potential vs. Hg/HgO (V)	Current density (mA cm^{-2})	Source
Pt/CNT/C 100 μg cm^{-2}	25	6	−0.2	125	[48]
			−0.5	520	
$Pr_{0.8}Ca_{0.2}MnO_3$/C 50 wt.%	60	8	−0.1	115	[144]
			−0.15	260	
CoTMPP/C Not known	25	5	−0.1	140	[71]
			−0.2	350	
			−0.25	500	
MnO_2/C 3.63 mg cm^{-2}	25	8	−0.2	91	[154]
			−0.5	440	
$LaMnO_3$/C 6.9 mg cm^{-2}	60	8	−0.08	300	[155]
			−0.1	400	
$MnCo_2O_4$/C 14 mg cm^{-2}	60	6	−0.1	150	[152]
			−0.2	300	

ment of increased AFC lifetimes. However, few studies have been reported in the literature to date.

3.9.1. CO_2 effect

Carbon dioxide is generally believed to be detrimental to the performance of the alkaline electrolyte due to the formation of carbonate species which will eventually cause a decrease in ionic conductivity. Thus, air is generally scrubbed to reduce the CO_2 content to between 5 and 30 ppm, depending on the technology used, before it enters the fuel cell [19]. However, residual CO_2 reacts to form carbonate ions following Eq. (1), which increases the ionic resistance of the KOH because the conductivity of CO_3^{2-} is lower than that of OH^-. If carbonate formation occurs, it forms in the pores of the electrode active layer. Subsequent mass transport will take place causing the carbonate species to be transferred to the bulk liquid electrolyte. If the wash out process, which depends on the porosity of the AL and the electrolyte viscosity, is fast enough, no CO_2 effect is observed; otherwise potassium carbonate is precipitated in the pores Eq. (2) blocking them, or causing destruction of the structure due to the expansion of the precipitate [156].

Authors are not unanimous on the effect of CO_2 on cathode degradation. Whereas Rolla [156] attributes CO_2 to be the main factor determining cathode ageing, Gulzow [157] has demonstrated 3500 h of operation with a cathode in the presence of CO_2 concentrations 150 times that in air, asserting that CO_2 in air had no influence on the cathode, but rather degradation in the fuel cell performance was attributed solely to its impact on electrolyte conductivity, which could be mitigated by exchanging the electrolyte every few hundreds hours (McLean estimates the KOH cost at 0.25 dollar cents/kWh if the electrolyte is changed every 500 h for a stack lifetime of 5000 h. Based on published evidence, the CO_2 effect seems to be electrode structure dependant, wherein the pore structure of the electrode is crucial. Sato observed a different CO_2 effect on the cathode stability depending on the carbon support used. It was found that CO_2 had a strong effect on cathode stability when electrodes were prepared from activated carbon. No CO_2 dissolution or progressive wetting was observed with Asahi-90 black which was explained by the small particle size of this carbon and its compact electrode structure [158].

3.9.2. Corrosion effect

The degradation reported by Tomantschger [159] of the electrochemical performance of the electrode with increasing operating time was assigned to the corrosion of carbon, and PTFE degradation caused by the KOH electrolyte. The carbon is slowly oxidized due to attack by the HO_2^- radical formed as an intermediate during oxygen reduction. Korovin [160] identified the discreet processes of electrocatalyst deterioration as composed of corrosion, chemical dissolution, cathode hydrogenization and metal intercalation. An increase in current density, temperature and ligand (OH^-) concentration was found to accelerate corrosion. A multi-catalyst system has been proposed to increase lifetime using the most stable support in a compromised conditions (medium electrolyte concentration, etc.). PTFE was shown to lose some hydrophobicity after

KOH exposure, which was attributed to surface chemical changes. It was shown that the contact angle reached a minimum; the higher the KOH temperature and concentration, the shorter the time taken to reach this minimum [161].

3.9.3. Weeping and flooding effects

The reduction of the cathode performance over time is often caused by flooding of the electrode structure by the electrolyte, which reduces oxygen accessibility to reacting sites by blocking gas pores. Gouerec [36] described this phenomenon as the main parameter driving cathode degradation, showing an increasing cell capacitance over time due to greater electrode surface being in contact with the electrolyte. Burchart [162] considered the role of electrocapillarity in which the contact angle between the electrode surface and the electrolyte is potential dependant. The contact angle was found to decrease with a decrease in potential from the OCV (open circuit voltage) which increased wetting of the electrode. An increase in pH and temperature, especially at 90 °C with the condensation of the vapour in gas pores, both lead to flooding of the electrode. Wagner [118] tested silver catalysed GDEs for 5000 h showing a voltage loss of 100 mV, which was partially explained by a decrease of the catalyst surface roughness, but mainly by PTFE degradation. The decrease in hydrophobicity with time allows more pore flooding, which hinders gas transport. The hypothesis that the degradation of cathode performance is mainly caused by excessive electrode wettability was confirmed by Maja [12] who showed that the use of acetylene black ensures a highly hydrophobic and homogeneous electrode structure with long term durability, whereas oil-furnace carbon such as Vulcan XC-72R displayed excessive wettability. Hull [163] and Baugh [164] studied the creep of alkaline electrolyte through cathodes. The production of OH^- ions arising from the ORR in the active zone increases its concentration. The movement of water from the bulk electrolyte, or from condensation via the vapour phase to compensate this gradient, causes an increase in the size of the active zone with the result that the reaction zone moves through the electrode. Khalidi [165] characterized the weeping process on the cathode and showed that humidification of the oxygen inlet reduces this effect.

4. Conclusions

AFCs offer a fuel cell solution with the potential for low cost. The alkaline electrolyte means that platinum based catalysts are not required, and AFC production methods are scaleable. AFC systems, which have been successfully used in space applications, need to meet the challenging requirement of low cost, high performance and durability to be successful in terrestrial applications. The development of circulating electrolyte systems has shown to have advantages compared to the immobilized electrolyte systems for terrestrial applications that could open the way to the commercialization of this technology. Electrolyte leakage and parasitic power losses are still challenges with the circulating electrolyte system and require the development of improved stack designs.

After a long hiatus in research and development, the alkaline fuel cell is creating renewed interest among research groups and some fuel cell companies, but research and development remains limited. There is no doubt that the success of this technology will come mainly by the improvement of electrodes, especially the cathode which is responsible for most of the cell losses.

Macro and micro structures in the different layers have to be obtained during the electrode fabrication to ally performance and durability where the carbon support is of prime importance in obtaining optimized performance. The development of new catalyst systems is more likely in alkaline media because of the wide range of options for the materials support and catalyst, as compared to acidic media which offers more limited materials choice. Alternatives to platinum have been investigated, showing good performance, comparable sometimes to platinum itself, but more work is needed to meet the durability targets required for commercial application.

References

[1] M.L. Perry, J. Electrochem. Soc. 149 (2002) S59.
[2] J.O.M. Bockris, A.J. Appleby, Energy 11 (1986) 95.
[3] G. Mulder, P. Coenen, A. Martens, J. Spaepen, Int. J. Hydrogen Energy 33 (2008) 3220–3224.
[4] M. Cifrain, K.V. Kordesch, in: W. Vielstich, A. Lamm, H. Gasteiger (Eds.), Handbook of Fuel Cells, vol 1, John Wiley, 2003, p. 267.
[5] M. Duerr, S. Gair, A. Cruden, J. McDonald, J. Power Sources 171 (2007) 1023–1032.
[6] E. Gulzow, M. Schulze, U. Gerke, J. Power Sources 156 (2006) 1–7.
[7] T. Hejze, J.O. Besenhard, K. Kordesch, M. Cifrain, R.R. Aronsson, J. Power Sources 176 (2008) 490–493.
[8] B.Y.S. Lin, D.W. Kirk, S.J. Thorpe, J. Power Sources 161 (2006) 474–483.
[9] A. Verma, S. Basu, J. Power Sources 168 (2007) 200–210.
[10] E. Gulzow, J. Power Sources 61 (1996) 99–104.
[11] G.F. McLean, T. Niet, S. Prince-Richard, N. Djilali, Int. J. Hydrogen Energy 27 (2002) 507–526.
[12] M. Maja, C. Orecchia, M. Strano, P. Tosco, M. Vanni, Electrochim. Acta 46 (2000) 423–432.
[13] A.E.S. Sleightholme, J.R. Varcoe, A.R. Kucernak, Electrochem. Commun. 10 (2008) 151–155.
[14] D. Stoica, L. Ogier, L. Akrour, F. Alloin, J.F. Fauvarque, Electrochim. Acta 53 (2007) 1596–1603.
[15] J.R. Varcoe, R.C.T. Slade, E.L.H. Yee, S.D. Poynton, D.J. Driscoll, J. Power Sources 173 (2007) 194–199.
[16] Y. Wang, L. Li, L. Hu, L. Zhuang, J. Lu, B. Xu, Electrochem. Commun. 5 (2003) 662–666.
[17] J.R. Varcoe, R.C.T. Slade (Eds.), Fuel Cells, Wiley-VCH, 2005, pp. 187–200.
[18] Y. Kiros, C. Myrén, S. Schwartz, A. Sampathrajan, M. Ramanathan, Int. J. Hydrogen Energy 24 (1999) 549–564.
[19] Y. Kiros, S. Schwartz, J. Power Sources 87 (2000) 101–105.
[20] M.A. Al-Saleh, J. Appl. Electrochem. 24 (1994) 575.
[21] M. Schulze, E. Gülzow, G. Steinhilber, Appl. Surface Sci. 179 (2001) 251–256.
[22] S. Gultekin, M.A. Al-Saleh, A.S. Al-Zakri, K.A.A. Abbas, Int. J. Hydrogen Energy 21 (1996) 485–489.
[23] T. Kenjo, Bull. Chem. Soc. Japan 54 (1981) 2553.
[24] K. Schultze, H. Bartelt, Int. J. Hydrogen Energy 17 (1992) 711–718.
[25] M.A. Al-Saleh, S. Gultekin, A.S. Al-Zakri, A.A.A. Khan, Int. J. Hydrogen Energy 21 (1996) 657–661.
[26] M.A. Al-Saleh, R. Sleem Ur, S.M.M.J. Kareemuddin, A.S. Al-Zakri, J. Power Sources 72 (1998) 159–164.
[27] J. Larminie, A. Dicks (Eds.), Fuel Cell Systems Explained, J. Wiley, 2002, pp. 109–122.
[28] M. Cifrain, K.V. Kordesch, J. Power Sources 127 (2004) 234–242.
[29] Fuel Cell Handbook, 7th ed., U.S. Dept. Energy, Morgantown, West Virginia, 2004.
[30] K. Kordesch, J. Gsellmann, M. Cifrain, S. Voss, V. Hacker, R.R. Aronson, C. Fabjan, T. Hejze, J. Daniel-Ivad, J. Power Sources 80 (1999) 190–197.
[31] T. Burchardt, P. Gouerec, E. Sanchez-Cortezon, Z. Karichev, J.H. Miners, Fuel 81 (2002) 2151–2155.
[32] E. De Geeter, M. Mangan, S. Spaepen, W. Stinissen, G. Vennekens, J. Power Sources 80 (1999) 207–212.
[33] K. Strasser, J. Power Sources 29 (1990) 149–166.
[34] K. Tomantschger, F. McClusky, L. Oporto, A. Reid, K. Kordesch, J. Power Sources 18 (1986) 317–335.
[35] E. Han, I. Eroglu, L. Turker, Int. J. Hydrogen Energy 25 (2000) 157–165.
[36] P. Gouerec, L. Poletto, J. Denizot, E. Sanchez-Cortezon, J.H. Miners, J. Power Sources 129 (2004) 193–204.
[37] Y. Kiros, S. Schwartz, J. Power Sources 36 (1991) 547–555.
[38] N.N.P. Brandon, D.D.J. Brett, Math. Phys.Eng. Sci. 364 (2006) 147–159.
[39] K. Tomantschger, K.V. Kordesch, J. Power Sources 25 (1989) 195–214.
[40] W.M. Vogel, K.A. Klinedinst, Electrochim. Acta 22 (1977) 1385–1388.
[41] K.A. Klinedinst, J. Mater. Sci. 11 (1976) 794.
[42] K.A. Klinedinst, J. Mater. Sci. 11 (1976) 209.
[43] A.L. Dicks, J. Power Sources 156 (2006) 128–141.
[44] J. Donnet, R. Bansal, M. Wang, Carbon Black, Marcel Dekker, 1993.
[45] T. Kyotani, Carbon 38 (2000) 269–286.
[46] K. Kinoshita, J.A.S. Bett, Carbon 11 (1973) 403–411.
[47] V. Hacker, E. Wallnofer, W. Baumgartner, T. Schaffer, J.O. Besenhard, H. Schrottner, M. Schmied, Electrochem. Commun. 7 (2005) 377–382.
[48] H. Huang, W. Zhang, M. Li, Y. Gan, J. Chen, Y. Kuang, J. Colloid Interf. Sci. 284 (2005) 593–599.
[49] C.-C. Yang, S.-T. Hsu, W.-C. Chien, M. Chang Shih, S.-J. Chiu, K.-T. Lee, C. Li Wang, Int. J. Hydrogen Energy 31 (2006) 2076–2087.

[50] A. Weidenkaff, S.G. Ebbinghaus, P. Mauron, A. Reller, Y. Zhang, A. Zuttel, Mater. Sci. Eng. C 19 (2002) 119–123.
[51] G.V. Shteinberg, A.V. Dribinsky, I.A. Kukushkina, L.N. Mokorousov, V.S. Bagotzky, J. Electroanal. Chem. 180 (1984) 619–637.
[52] G.V. Shteinberg, A.V. Dribinsky, I.A. Kukushkina, M. Musilova, J. Mrha, J. Power Sources 8 (1982) 17–33.
[53] Y. Kiros, T. Quatrano, P. Bjornbom, Electrochem. Commun. 6 (2004) 526–530.
[54] K.J. Euler, J. Appl. Electrochem. 2 (1972) 105.
[55] K. Mund, F.v. Sturm, Electrochim. Acta 20 (1975) 463–467.
[56] N. Giordano, E. Passalacqua, V. Alderucci, P. Staiti, L. Pino, H. Mirzaian, E.J. Taylor, G. Wilemski, Electrochim. Acta 36 (1991) 1049–1055.
[57] L.G. Austin, Ind. Eng. Chem. Fundam. 4 (1965) 321.
[58] S. Srinivasan, H.D. Hurwitz, Electrochim. Acta 12 (1967) 495–512.
[59] V.S. Markin, Russian Chem. Bull. 12 (1963) 1551.
[60] E.A. Grens, Electrochim. Acta 15 (1970) 1047–1057.
[61] E.A. Grens, C.W. Tobias, Electrochim. Acta 10 (1965) 761–772.
[62] J. Giner, J. Electrochem. Soc. 116 (1969) 1124.
[63] R.P. Iczkowski, J. Electrochem. Soc. 127 (1980) 1433.
[64] W. Vogel, J. Lundquist, A. Bradford, Electrochim. Acta 17 (1972) 1735–1744.
[65] S.-C. Yang, P. Bjornbom, Electrochim. Acta 37 (1992) 1831–1843.
[66] J.H. Jo, J. Appl. Electrochem. 30 (2000) 1023.
[67] M.C. Kimble, J. Electrochem. Soc. 138 (1991) 3370.
[68] M.C. Kimble, J. Electrochem. Soc. 139 (1992) 478.
[69] T. Kenjo, K. Kawatsu, Electrochim. Acta 30 (1985) 229–233.
[70] M.T. Ergul, L. Turker, I. Eroglu, Int. J. Hydrogen Energy 22 (1997) 1039–1045.
[71] J. Kivisaari, J. Lamminen, M.J. Lampinen, M. Viitanen, J. Power Sources 32 (1990) 233–241.
[72] K. Kordesch, S. Jahangir, M. Schautz, Electrochim. Acta 29 (1984) 1589–1596.
[73] D.M. Drazic, R.R. Adzic, Electrochim. Acta 14 (1969) 405–411.
[74] R. Manoharan, A.K. Shukla, J. Power Sources 10 (1983) 333–341.
[75] A.J. Appleby, M. Savy, J. Electroanal. Chem. 92 (1978) 15–30.
[76] M. Pirjamali, Y. Kiros, J. Power Sources 109 (2002) 446–451.
[77] K. Kordesch, V. Hacker, J. Gsellmann, M. Cifrain, G. Faleschini, P. Enzinger, R. Fankhauser, M. Ortner, M. Muhr, R.R. Aronson, J. Power Sources 86 (2000) 162–165.
[78] M. Musilova, A. Kaisheva, J. Mrha, I. Iliev, S. Gamburzev, J. Power Sources 3 (1978) 245–255.
[79] S. Motoo, M. Watanabe, N. Furuya, J. Electroanal. Chem. 160 (1984) 351–357.
[80] M. Watanabe, K. Makita, H. Usami, S. Motoo, J. Electroanal. Chem. 197 (1986) 195–208.
[81] M. Watanabe, M. Tomikawa, S. Motoo, J. Electroanal. Chem. 182 (1985) 193–196.
[82] A.J. Appleby, J. Electroanal. Chem. 357 (1993) 117–179.
[83] E. Yeager, Electrochim. Acta 29 (1984) 1527–1537.
[84] N.M. Markovic, et al., J. Electrochem. Soc. 144 (1997) 1591.
[85] K.F. Blurton, E. McMullin, Energy Conv. 9 (1969) 141–144.
[86] B.B. Blizanac, P.N. Ross, N.M. Markovic, Electrochim. Acta 52 (2007) 2264–2271.
[87] N.A. Anastasijevic, Z.M. Dimitrijevic, R.R. Adzic, J. Electroanal. Chem. 199 (1986) 351–364.
[88] G. Bianchi, F. Mazza, T. Mussini, Electrochim. Acta 7 (1962) 457–473.
[89] J.M. Martinovic, D.B. Sepa, M.V. Vojnovic, A. Damjanovic, Electrochim. Acta 33 (1988) 1267–1272.
[90] J.M. Martinovic, D.B. Sepa, M.V. Vojnovic, A. Damjanovic, Electrochim. Acta 34 (1989) 671–676.
[91] R. Pattabiraman, Appl. Catal. A: Gen. 153 (1997) 9–20.
[92] D.B. Sepa, M.V. Vojnovic, M. Stojanovic, A. Damjanovic, J. Electroanal. Chem. 218 (1987) 265–272.
[93] D.B. Sepa, M.V. Vojnovic, L.M. Vracar, A. Damjanovic, Electrochim. Acta 32 (1987) 129–134.
[94] W.M. Vogel, Electrochim. Acta 13 (1968) 1821–1826.
[95] Y.-F. Yang, Y.-H. Zhou, C.-S. Cha, Electrochim. Acta 40 (1995) 2579–2586.
[96] F.H.B. Lima, E.A. Ticianelli, Electrochim. Acta 49 (2004) 4091–4099.
[97] K.V. Ramesh, A.K. Shukla, J. Power Sources 19 (1987) 279–285.
[98] M. Chatenet, J. Electrochem. Soc. 150 (2003) D47.
[99] G. Couturier, D.W. Kirk, P.J. Hyde, S. Srinivasan, Electrochim. Acta 32 (1987) 995–1005.
[100] M.-k. Min, J. Cho, K. Cho, H. Kim, Electrochim. Acta 45 (2000) 4211–4217.
[101] T. Toda, H. Igarashi, M. Watanabe, J. Electroanal. Chem. 460 (1999) 258–262.
[102] M.B. Vukmirovic, J. Zhang, K. Sasaki, A.U. Nilekar, F. Uribe, M. Mavrikakis, R.R. Adzic, Electrochim. Acta 52 (2007) 2257–2263.
[103] N. Giordano, E. Passalacqua, V. Recupero, M. Vivaldi, E.J. Taylor, G. Wilemski, Electrochim. Acta 35 (1990) 1411–1421.
[104] K. Sasaki, Y. Mo, J.X. Wang, M. Balasubramanian, F. Uribe, J. McBreen, R.R. Adzic, Electrochim. Acta 48 (2003) 3841–3849.
[105] J.J. Zhang, M.B.M.B. Vukmirovic, Y.Y. Xu, M.M. Mavrikakis, R.R.R.R. Adzic, Angew. Chem. (Int. Ed.) 44 (2005) 2132–2135.
[106] V.S. Bagotzky, E.I. Khrushcheva, M.R. Tarasevich, N.A. Shumilova, J. Power Sources 8 (1982) 301–309.
[107] Y. Kiros, J. Electrochem. Soc. 143 (2005) 2152.
[108] L. Dubau, J. Appl. Electrochem. 33 (2003) 419.
[109] L. Dubau, F. Hahn, C. Coutanceau, J.M. Leger, C. Lamy, J. Electroanal. Chem. 554–555 (2003) 407–415.
[110] R. Kotz, E. Yeager, J. Electroanal. Chem. 111 (1980) 105–110.
[111] M. Chatenet, L. Genies-Bultel, M. Aurousseau, J. Appl. Electrochem. 32 (2002) 1131–1140.
[112] L. Demarconnay, C. Coutanceau, J.M. Leger, Electrochim. Acta 49 (2004) 4513–4521.
[113] D.J. Guo, H.L. Li, Carbon 43 (2005) 1259–1264.
[114] H.-K. Lee, J.-P. Shim, M.-J. Shim, S.-W. Kim, J.-S. Lee, Mater. Chem. Phys. 45 (1996) 238–242.
[115] N.D. Merkulova, G.V. Zhutaeva, N.A. Shumilova, V.S. Bagotzky, Electrochim. Acta 18 (1973) 169–174.
[116] N.A. Shumilova, G.V. Zhutaeva, M.P. Tarasevich, Electrochim. Acta 11 (1966) 967–974.
[117] K. Smrcek, J. Power Sources 7 (1981) 105–112.
[118] N. Wagner, M. Schulze, E. Gulzow, J. Power Sources 127 (2004) 264–272.
[119] Y. Yang, Y. Zhou, J. Electroanal. Chem. 397 (1995) 271–278.
[120] K. Smrcek, J. Beran, J. Jandera, J. Power Sources 2 (1978) 273–286.
[121] J. Mrha, I. Iliev, A. Kaisheva, S. Gamburzev, M. Musilova, J. Power Sources 1 (1976) 47–56.
[122] M. Appel, A.J. Appleby, Electrochim. Acta 23 (1978) 1243–1246.
[123] I. Iliev, J. Mrha, A. Kaisheva, S. Gamburzev, J. Power Sources 1 (1976) 35–46.
[124] A. Verma, A.K. Jha, S. Basu, J. Power Sources 141 (2005) 30–34.
[125] I. Roche, J. Phys. Chem. 111 (2007) 1434.
[126] J. Yang, J.J. Xu, Electrochem. Commun. 5 (2003) 306–311.
[127] M.L. Calegaro, F.H.B. Lima, E.A. Ticianelli, J. Power Sources 158 (2006) 735–739.
[128] F.H.B. Lima, M.L. Calegaro, E.A. Ticianelli, J. Electroanal. Chem. 590 (2006) 152–160.
[129] F.H.B. Lima, M.L. Calegaro, E.A. Ticianelli, Electrochim. Acta 52 (2007) 3732–3738.
[130] L. Mao, Electrochim. Acta 48 (2003 1015).
[131] K. Arihara, J. Electrochem. Soc. 151 (2004) A2047.
[132] D. Zhang, D. Chi, T. Okajima, T. Ohsaka, Electrochim. Acta 52 (2007) 5400–5406.
[133] Y.L. Cao, H.X. Yang, X.P. Ai, L.F. Xiao, J. Electroanal. Chem. 557 (2003) 127–134.
[134] K. Matsuki, Electrochim. Acta 31 (1986) 13.
[135] A. Elzing, A. van der Putten, W. Visscher, E. Barendrecht, J. Electroanal. Chem. 200 (1986) 313–322.
[136] S. Sarangapani, P. Lessner, M. Manoukian, J. Giner, J. Power Sources 29 (1990) 437–442.
[137] Y. Kiros, O. Lindstrom, T. Kaimakis, J. Power Sources 45 (1993) 219–227.
[138] C. Mocchi, S. Trasatti, J. Mol. Catal. A: Chem. 204–205 (2003) 713–720.
[139] H. Tributsch, U.I. Koslowski, I. Dorbandt, Electrochim. Acta 53 (2008) 2198–2209.
[140] V. Hermann, D. Dutriat, S. Muller, C. Comninellis, Electrochim. Acta 46 (2000) 365–372.
[141] R. Manoharan, A.K. Shukla, Electrochim. Acta 30 (1985) 205–209.
[142] A. Weidenkaff, S.G. Ebbinghaus, T. Lippert, M.J. Montenegro, C. Soltmann, R. Wessicken, Cryst. Eng. 5 (2002) 449–457.
[143] Y. Kiros, C. Myren, S. Schwartz, A. Sampathrajan, M. Ramanathan, Int. J. Hydrogen Energy 24 (1999) 549–564.
[144] T. Hyodo, M. Hayashi, S. Mitsutake, N. Miura, J. Appl. Electrochem. 27 (1997).
[145] M. Bursell, M. Pirjamali, Y. Kiros, Electrochim. Acta 47 (2002) 1651–1660.
[146] J. Ortiz, J.L. Gautier, J. Electroanal. Chem. 391 (1995) 111–118.
[147] E. Rios, H. Reyes, J. Ortiz, J.L. Gautier, Electrochim. Acta 50 (2005) 2705–2711.
[148] A. Restovic, E. Rios, S. Barbato, J. Ortiz, J.L. Gautier, J. Electroanal. Chem. 522 (2002) 141–151.
[149] R.N. Singh, J.P. Pandey, N.K. Singh, B. Lal, P. Chartier, J.F. Koenig, Electrochim. Acta 45 (2000) 1911–1919.
[150] T. Nissinen, Y. Kiros, M. Gasik, M. Lampinen, Mater. Res. Bull. 39 (2004) 1195–1208.
[151] T. Nissinen, M. Leskela, M. Gasik, J. Lamminen, Electrochim. Acta 427 (2005) 155–161.
[152] T. Nissinen, T. Valo, M. Gasik, J. Rantanen, M. Lampinen, J. Power Sources 106 (2002) 109–115.
[153] K.V. Ramesh, P.R. Sarode, S. Vasudevan, A.K. Shukla, J. Electroanal. Chem. 223 (1987) 91–106.
[154] C.-C. Yang, Int. J. Hydrogen Energy 29 (2004) 135–143.
[155] M. Hayashi, H. Uemura, K. Shimanoe, J. Electrochem. Soc. 151 (2004) A158.
[156] A. Rolla, A. Sadkowski, J. Wild, P. Zoltowski, J. Power Sources 5 (1980) 189–196.
[157] E. Gulzow, M. Schulze, J. Power Sources 127 (2004) 243–251.
[158] M. Sato, M. Ohta, M. Sakaguchi, Electrochim. Acta 35 (1990) 945–950.
[159] K. Tomantschger, R. Findlay, M. Hanson, K. Kordesch, S. Srinivasan, J. Power Sources 39 (1992) 21–41.
[160] N.V. Korovin, Electrochim. Acta 39 (1994) 1503–1508.
[161] Y. Rotenberg, S. Srinivasan, E.I. Vargha-Butler, A.W. Neumann, J. Electroanal. Chem. 213 (1986) 43–51.
[162] T. Burchardt, J. Power Sources 135 (2004) 192–197.
[163] M. Hull, H. James, J. Electrochem. Soc. 124 (1977) 332.
[164] L. Baugh, J. Cook, J. Lee, J. Appl. Electrochem. 8 (1978) 253.
[165] A. Khalidi, B. Lafage, P. Taxil, G. Gave, M.J. Clifton, P. Cezac, Int. J. Hydrogen Energy 21 (1996) 25–31.